SUB-SURFACE DAMAGE LOCATION AND IDENTIFICATION USING INFRA-RED TECHNIQUES

T.R. Emery[1], J. M. Dulieu-Barton[1], P.R. Cunningham[2]
[1]University of Southampton, School of Engineering Sciences, SO17 1BJ, UK
[2] Loughborough University, Department of Aeronautical and Automotive Engineering, LE11 3TU, UK,
p.cunningham@lboro.ac.uk

SUMMARY

The paper presents a new methodology for identifying sub-surface damage in composite components using a combination of Pulse Phase Thermography (PPT) and Thermoelastic Stress Analysis (TSA).

*Keywords: Composite structures, **T**hermoelastic **S**tress **A**nalysis (TSA), **P**ulsed **P**hase **T**hermography (PPT), Damage*

INTRODUCTION

The location and identification of damage in composite materials is currently a topic of considerable interest, and many techniques are being applied and developed in both the research and industrial communities in order to advance knowledge in the area. Infra-red thermography (IRT) systems are now available that can collect data a high rates and allow the heating effects due to damage to be observed in real time. Thermoelastic Stress Analysis (TSA) [1] is a non-contacting, full-field measurement technique that uses IRT as its basis and has been shown to have great potential for use in damage assessment studies. In TSA, IRT is used to obtain the small temperature change that occurs as a result of a strain change in the structure. It is now possible to monitor the evolution of damage in real time using TSA. It is also possible to decouple the part of the thermoelastic response caused by heating at the damage site from the response produced by the strain change [2]. Therefore TSA can now be applied as a quantitative tool for damage assessment. The difficulty with TSA is that it is essentially a surface technique and in many cases damage evolves from subsurface defects and/or delaminations. Pulse Phase Thermography (PPT) is a relatively new approach that combines pulse and modulated thermography [3]. The main advantage of the PPT approach is that it has the potential to reveal sub-surface damage. It is also portable, so that inspections of components that are in-service can take place. Furthermore it is relatively fast, so that inspections of large components can be carried out to pin-point areas of damage for further analysis, using a technique such as TSA. The purpose of this paper is to define a methodology where PPT is used to detect, locate and identify the extent of sub-surface delamination damage and then TSA is used to characterise the effect of the damage on the stress field in the component.

Thermoelastic Stress Analysis

TSA is an experimental technique that is based on the well documented thermoelastic effect, e.g. [4, 5]. The technique uses a highly sensitive infra-red (IR) detector to measure the small temperature changes (of the order of mK) within the field of view that can in turn be related to the change in the sum of the principal stresses $\Delta(\sigma_x + \sigma_y)$, as follows:

$$\Delta T = \frac{\alpha T}{\rho C_p} \Delta(\sigma_x + \sigma_y) \quad (1)$$

where α is the coefficient of linear thermal expansion, T is the absolute temperature, ρ is the density and C_p is the specific heat at constant pressure.

The analogue output from the IR detector is digitally processed into the thermoelastic signal (S) and is related to the change in the sum of the principal stresses using a calibration constant (A) which can be experimentally determined [6], as follows [7]:

$$\Delta(\sigma_x + \sigma_y) = AS \quad (2)$$

Equation (2) is applicable for an isotropic homogeneous material. Orthotropic materials have markedly different mechanical properties in the principal material directions and consequently the simple thermoelastic theory devised for an isotropic body is not valid for orthotropic composite materials [8]. The thermoelastic theory has been developed [8] into an equation for an orthotropic homogeneous material as follows:

$$(\alpha_1 \Delta\sigma_1 + \alpha_2 \Delta\sigma_2) = A^* S \quad (3)$$

where α_1 and α_2 are the coefficients of linear thermal expansion in the principal material directions, $\Delta\sigma_1$ and $\Delta\sigma_2$ are the changes in the direct surface stresses in the principal material directions and A^* is an orthotropic calibration constant.

The technique has not been widely applied to the assessment of composite structures due to the difficulties presented by the material anisotropic behaviour. However, with recent developments in the instrumentation, that has allowed more detailed data to be gathered in virtually real time, the incentive to apply TSA to damage studies of composite components has been provided. Through calibration of the signal, the output can be related to the stresses in the structure and therefore life assessments may be possible.

Equation (3) is developed [8] in terms of the principal surface stresses. To calibrate the thermoelastic theory it is therefore necessary to obtain values of the surface stress. In laminated composite materials this can be achieved by applying classical laminate theory (CLT) provided the elastic properties of the lamina, the thickness of the manufactured plies and the loads are known. This can provide a route to calibration [9] based on Equation (3) but is laden with possible sources of error due to estimates of material properties etc. A better approach is to formulate Equation (3) in terms of strain, which leads to:

$$A * S = (\alpha_1 Q_{11} + \alpha_2 Q_{12})\Delta\varepsilon_1 + (\alpha_1 Q_{12} + \alpha_2 Q_{22})\Delta\varepsilon_2 \quad (4)$$

where α_1 and α_2 are the coefficients of thermal expansion in the surface lamina relative fibre directions, Q_{11}, Q_{12}, and Q_{22} are the laminate reduced stiffness terms [10], and $\Delta\varepsilon_1$ and $\Delta\varepsilon_2$ are the surface lamina strains in the relative fibre directions. This equation can also be rewritten in terms of the strains in the laminate principal material directions (L and T directions) using the strain transformation equations [10].

This formulation provides a direct approach to calibration, as the strain is constant through the thickness of a laminate and furthermore can be measured using extensometers or strain gauges.

Pulse Phase Thermography

PPT is a relatively new approach that combines the traditional IRT techniques of pulse (PT) and modulated thermography (MT) [11]. It is a *passive* technique and therefore can be applied to large areas of in-service composite structures. Furthermore, it is relatively fast, so that inspections of large components can be carried out to pin-point areas of damage for further analysis. PPT is achieved by subjecting the structure under evaluation to a pulse of heat energy that propagates through the structure and subsequently analysing the thermal signature from the surface. A sequence of IR images is collected from the surface following the thermal pulse that captures the thermal decay *T(t)*. Mathematically the thermal pulse can be decomposed into a multitude of individual sinusoidal components [11] with various amplitudes and frequencies. The frequency content of these sinusoidal components, that diffuse through the structure and appear on the surface, can be obtained from the thermal images recorded using Fourier transformation analysis. The extraction and comparison of various specified frequency ranges, using a discrete one-dimensional Fourier transform at each pixel in the image, provides the basis for PPT. The frequency range analysed is dependent on the damage location and geometry within the specimen. The output is provided in terms of the amplitude and phase of the frequency wave at the surface. The output is referenced relative to each pixel, at time *t*, in the field of view and as such no reference input is required but any change in transmission evident at the surface can be evaluated. Phase lag or attenuation, of the wave in question, at a pixel relative to another pixel will be evident in the analysis of the results. Any deviation in the phase or amplitude results is assumed to be apparent as a consequence of the specific diffusion path. The diffusion through the structure is influenced by the thermal conductivity, which will be modified at damage sites such as delaminated areas. Hence the heat diffusion through the damage will be modified and data from this region will have a different phase to that from undamaged material. Therefore, the damaged region will be revealed as a deviation in a phase plot.

METHODOLOGY

Test Specimen Design

The test specimens were manufactured using SP Systems SE84 pre-impregnated UD E-glass epoxy material, with various lay-up configurations, details of which are given later in this paper. Each test specimen was 295mm long, 100mm wide, and 1.5mm thick, and the material properties for the individual GFRP layers is given in Table 1.

Table 1. UD E-Glass/epoxy material properties

Longitudinal Young's modulus, E_1	36.8 GPa (Measured)
Transverse Young's modulus, E_2	8.4 GPa (Measured)
Shear modulus, G_{12}	3 GPa [10]
Major Poisson's ratio, ν_{12}	0.25 (Measured)
Minor Poisson's ratio, ν_{21}	0.05 (Measured)
Coefficient of thermal expansion, α_1	$6\times10^{-6}/\,°C$ [18]
Coefficient of thermal expansion, α_2	$35\times10^{-6}/\,°C$ [18]

Fatigue Rig

The fatigue rig was based on a design reported [12] in which a rig was developed to propagate delamination damage for acoustic fatigue studies of CFRP. The purpose of the rig was to generate interlaminar shear between neighbouring plies within the laminate. A servo hydraulic test machine was used to apply the displacement therefore the fatigue rig was designed to be mounted directly to the test machine as shown in Figure 1. The displacement of the free end of the test specimen is achieved though a roller which does not subject the laminate to a point load but generates a pure bending moment. The plan elevation in Figure 1 illustrates the clamped boundary condition designed in a half sine profile as suggested in [12]. The purpose of this clamp design is to generate higher levels of interlaminar shear in the central region of the laminate and helps initiates delamination damage away from the free-edges. Further, this avoids peeling at the free-edges of the specimen and the arrangement ensures fatigue damage initiates along the centreline.

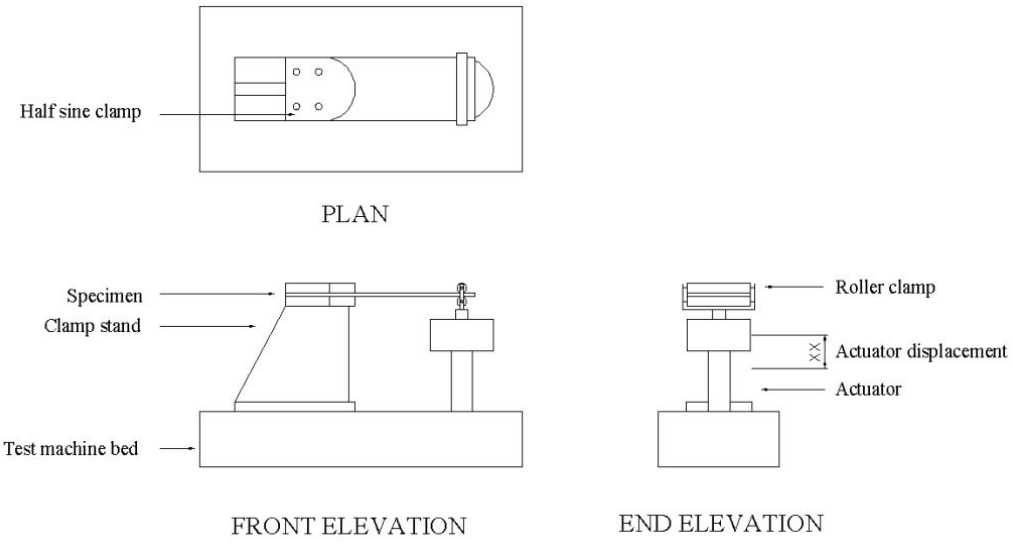

Figure 1. Fatigue rig in-situ on servo-hydraulic test machine.

Fatigue Test Routine and Experimental Procedure

Figure 2a shows a laminate in the undamaged condition. For reference Figure 2b shows a UD specimen with PTFE inserts as used in [13]. As the specimens are made of GFRP, it is possible to see the PTFE and also allows any damage to be visually observed in the specimen during fatigue.

The first laminate to be fatigue loaded was manufactured with a stacking sequence of $[0, 45, -45]_s$ and was subjected to 37800 cycles of fully reversed bending

with a displacement amplitude of 30 mm at 1 Hz. Visual inspection of the specimen revealed delamination had propagated, the extent of the damage can be seen in Figure 2c and 2d. The visual images were obtained using a digital camera and illuminating the rear of the specimen. The delamination damage achieved can be appreciated when compared to the as manufactured laminate and the laminate with pseudo delamination inserts.

To reduce the number of fatigue cycles in which delamination may be initiated and propagated in laminates it was decided to manufacture specimens with stacking sequences that generated a greater shear coupling ply mismatch. This was because it has been reported that the shear stress generated in angle-ply laminates can have a strong influence on delamination [14]. The peak mismatch in the shear coupling coefficient occurs when the plies are orientated at about ± 20˚ [15]. As expected there is no mismatch in the shear coupling coefficient for cross ply laminates as the coefficient tends to zero when the plies are orientated at 0˚ and 90˚.

Therefore a laminate was manufactured with a stacking sequence of $[0, 25, -25]_s$ and was subjected to 19600 cycles at 25mm displacement amplitude. The damaged laminate is shown Figure 2e and 2f and show that a significant delamination can be achieved over a much reduced fatigue period than that of the initial $[0, 45, -45]_s$ specimen. A further factor to consider is in Figure 2c, 2d, 2e and 2f surface cracking has occurred that is a result of the clamp corners causing damage to the surface plies. The clamp corners were rounded to prevent the surface damage.

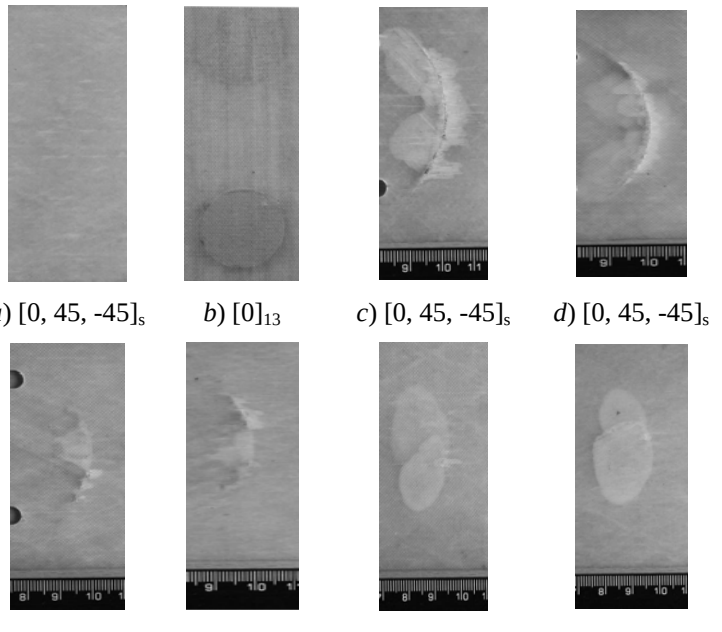

a) $[0, 45, -45]_s$ *b*) $[0]_{13}$ *c*) $[0, 45, -45]_s$ *d*) $[0, 45, -45]_s$

e) $[0, 25, -25]_s$ *f*) $[0, 25, -25]_s$ *g*) $[0, 25,-25, 0]_s$ *h*) $[0, 25,-25, 0]_s$

Figure 2. Delaminated GFRP specimens.

The last laminate maintained the ± 25˚ angle plies within the laminate but they were separated by two 0 ˚ plies in the centre of the laminate which moved the angled plies away from the neutral axis of the laminate, resulting in a $[0, 25, -25, 0]_s$ laminate. The laminate was cycled for 19600 cycles again with 25 mm displacement amplitude. Figure 2g and 2h illustrate the delamination that was achieved. Inspection of Figure 2g and 2h (from the front and rear surface respectively) show that the delamination occurs

at two spatial locations through the laminate thickness; 1) between the first ± 25˚ laminae and 2) repeated between the second ± 25˚ laminae, i.e. between the 2nd and 3rd lamina and the 7th and 8th lamina from the surface ply.

RESULTS AND DISCUSSION

Pulsed Phase Thermography

To establish the extent of the damage PPT was performed on the specimen at the end of the fatigue test routine, in reality this would determine the area that the TSA would be directed. The specimen was clamped in a vertical orientation and subjected to a metered thermal pulse using a Cullman camera flash unit positioned in contact with the rear surface of the specimen. A Cedip Silver 450M IR system was positioned 0.5 m from the front surface of the specimen and collected thermal data during the temperature decay from the surface. The basis of the set-up followed recommendations of Marinetti *et al.* [16]. The temporal information from the sequence of 500 thermal frames recorded was analysed for the frequency content of the constituent wave forms using a Fourier transform algorithm provided in the Cedip Altair software. The frequency range over which the analysis was carried out was between 0.1 and 1 Hz. The resolution of the results was determined by the frequency increment which was set at 0.09 Hz and thus provided 11 groups.

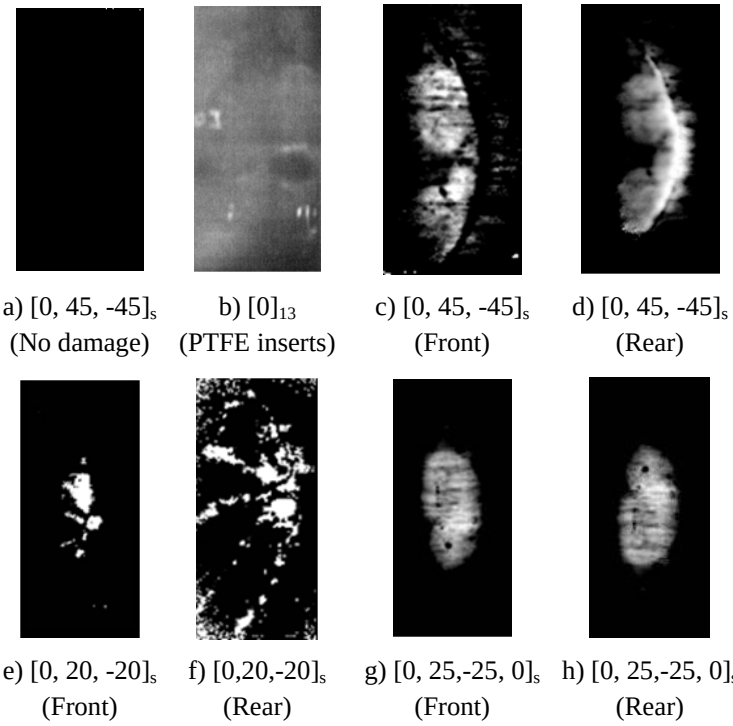

a) $[0, 45, -45]_s$ (No damage) b) $[0]_{13}$ (PTFE inserts) c) $[0, 45, -45]_s$ (Front) d) $[0, 45, -45]_s$ (Rear)

e) $[0, 20, -20]_s$ (Front) f) $[0,20,-20]_s$ (Rear) g) $[0, 25,-25, 0]_s$ (Front) h) $[0, 25,-25, 0]_s$ (Rear)

Figure 3. PPT results from delaminated specimens.

The defect visible in Figure 3 is provided as a function of the phase difference of a 0.5 Hz frequency wave set. The defect is visible as a result of the modification of the diffusion path, due to the damage altering the thermal conductivity, from the energy source to the surface. (The delamination is essentially an air pocket and modifies the

diffusion characteristics so that the damage could be visualised using the PPT technique). The phase reference is taken across the field of view with respect to the defect area. It can be seen that the defects revealed using PPT correlate well with the visual inspections in Figure 2. In all cases where delamination is present it can be seen that the PPT routine is capable of discerning the spatial extent of the subsurface damage.

TSA damage analysis

The thermoelastic damage analysis was conducted by obtaining thermoelastic data from the damaged laminate in the fatigue rig (Figure 1) and using the actuator displacement to cyclically load the laminate. A Deltatherm system was used to collect this data, which introduces a challenge as the laminate cannot be positioned directly in the field of view. The DeltaTherm system cannot be positioned above the fatigue rig as it must be maintained in a horizontal position due to the open storage of liquid nitrogen that is used to cool the IR detector. In [17] it was reported that a mirror could be used to collect thermoelastic data where a component was loaded horizontally; although a small reduction in the signal of 7.2 % was reported. As the attenuation is constant throughout the testing it could be incorporated in a calibration routine if necessary. The set-up for the fatigue rig is shown in Figure 4.

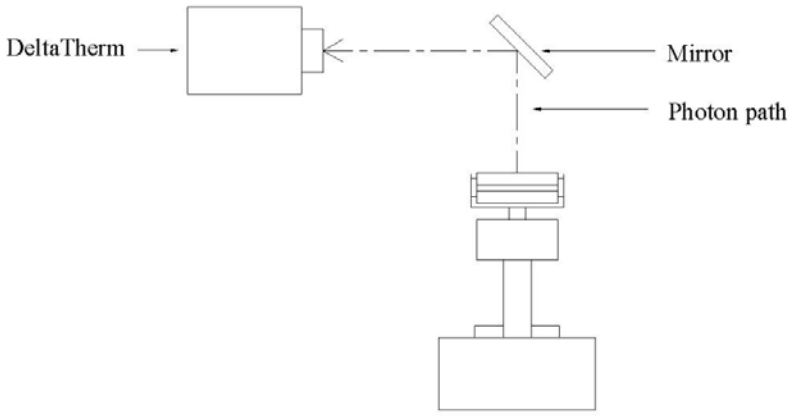

Figure 4. TSA test set-up.

The first laminate tested was the $[0, 25,-25, 0]_s$ specimen which was cyclically displaced at 1.3 mm at 10 Hz frequency and thermoelastic data collected. The expected stress distribution due to the clamping arrangement and the bending moment applied was clearly evident in the uncalibrated thermoelastic data however it was not possible to obtain thermoelastic results that indicated any deviation in the surface stress at the known location of the subsurface damage. Thermoelastic data was also collected from the $[0, 20, -20]_s$ and $[0, 45, -45]_s$ laminates (which had been delaminated) which were also loaded at the same amplitude and frequency; the thermoelastic data depicted the gross surface cracking but provided no further indication of the subsurface damage.

There are a number of reasons why the thermoelastic data did not display any variation in the signal around the delaminated area. Firstly, the delamination damage is located near the central axis of the laminate which under bending is a neutral axis and as such the damage may not effect the strain distribution within the laminate. Secondly, at 10 Hz the applied displacement amplitude was restricted to 1.3mm which may not cause

sufficient strain within the laminate for the damage to modify the strain distribution at the surface. It may be possible to overcome both problems by manufacturing a thicker laminate thereby allowing the angle plies to be moved further from the central axis and this would also result in a larger stress within the laminate for the achievable displacement amplitude at the required frequency. In response to the questions raised [13] during the attempt to observe pseudo delamination damage using TSA it was decided that a specimen could be fatigued in the rig and subject to TSA in uniaxial tension-tension loading. As the existence of delamination damage could be verified it would be possible to assess the response of TSA to delamination damage alone from a specimen subjected to a tensile load. To enable the specimen to be loaded between the grips of the servo-hydraulic test machine a narrower specimen of 45 mm width was manufactured. The specimen was subject to fatigue and TSA loading as detailed in Table 2.

Table 2. Cyclic loading

Specimen	TSA		Fatigue			
	Displacement	Frequency	Displacement	Frequency	Cycles	Number of steps
i)	0.167 mm	10 Hz	20 mm	1 Hz	6000	5

For consistency however the specimen was cyclically loaded using a constant displacement and this would allow for any unanticipated reduction in stiffness. Initial thermoelastic data was obtained before the specimen was fatigued and is shown in Figure 5a. Within the noise level expected the thermoelastic data recorded is uniform across the surface. The specimen was fatigued as detailed in Table 2 over 5 steps of approximately 6000 cycles or at a stage when it was evident that damage had visibly propagated. The data in Figure 5b, 5c, 5d and 5e show influence of the progression of the damage on the thermoelastic signal and compares to the damaged area seen in the visual image in Figure 5f which shows the damage evident at the end of the test.

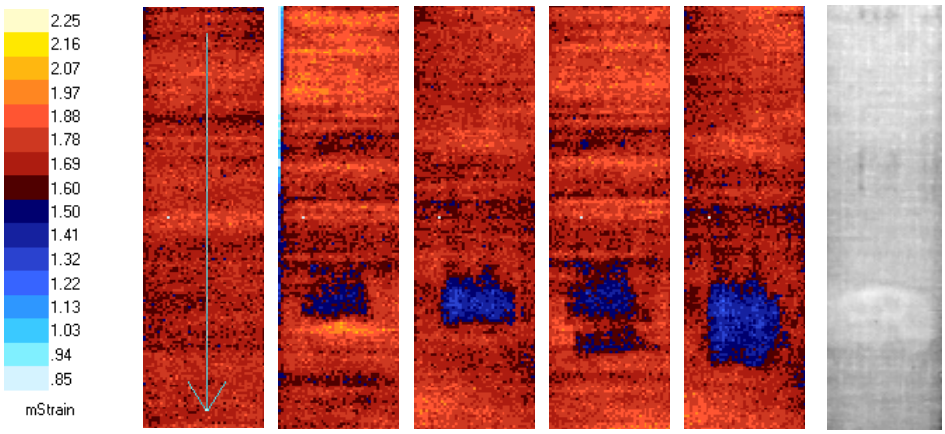

$(\Delta\varepsilon_L + \Delta\varepsilon_T)$ a) b) Step 1 c) Step 2 d) Step 3 e) Step 4 f) Visual

Figure 5. Thermoelastic signal from specimen through fatigue history.

The strain data for the delaminated specimen was analysed using a ‘damage analysis’ macro [15], which was written in MATLAB to provide a percentage change in the strain sum between undamaged and damaged specimen data. Two data sets are

compared; one from the step 1 (Figure 5b) and the other from the undamaged state (Figure 5a).

The results are shown in Figure 6; the full-field contour plot shows the regions that are affected by the subsurface delamination and in Figure 6b a line plot (as defined in Figure 5a) plots the data interrogated along the line. There are two regions of interest, from pixel 82 to 104, where the signal has increased/decreased significantly. Through the area corresponding to the delaminated region the signal is reduced by a factor of 0.8. At the delamination front there is a concentrated region of high signal 1.17 times greater than that recorded form the undamaged specimen. A further area of signal change has occurred due to the fatigue away from the delaminated area, this is located between pixels 19 to 27. This area corresponds to the section of the strip located between the rollers of the fatigue rig where damage has also accumulated. The comparison of the thermoelastic data collected from the undamaged and damaged structure demonstrates the capability of TSA to provide information on strain redistribution caused by subsurface damage.

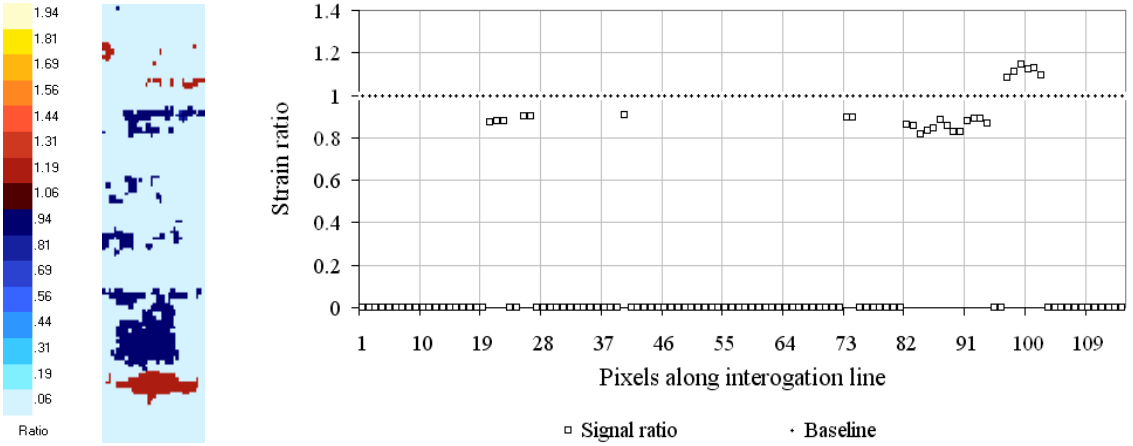

a) b)

Figure 6. Thermoelastic damage analysis ratio.

CONCLUSIONS

A methodology has been presented to permit the integrity assessment of composite structure subject damage using two IR techniques (PPT and TSA) to provide a non-contact, non-destructive and full-field damage assessment. This has been demonstrated on a GFRP specimen with delamination damage. A visualisation procedure highlighted the areas containing gross damage and has the potential to isolate regions were repair is necessary.

ACKNOWLEDGEMENTS

The authors gratefully acknowledge the Engineering and Physical Sciences Research Council for the loan of some of the IR equipment.

References

1. Dulieu-Barton, J.M., and Stanley, P., *Development and applications of thermoelastic stress analysis*, J. Strain Analysis, 1998, 33, 93-104.

2. Dulieu-Barton J.M., Emery T.R., Quinn S., Cunningham P.R., *A temperature correction methodology for quantitative thermoelastic stress analysis and damage assessment*, Meas. Sci. Tech., 2006, 17 ,1627-1637.
3. S. Marinetti, Y.A. Plotnikov, W.P. Winfree and A. Braggiotti, *Pulse phase thermography for defect detection and visualization*, Nondestructive Evaluation of Aging Aircraft, Airports, and Aerospace Hardware III, SPIE 1999.
4. Pitarresi, G. and Patterson, E. A., A review of the general theory of thermoelastic stress analysis. *The Journal of Strain Analysis for Engineering Design*, 2003, 38 (5), 405-417.
5. Stanley, P. and Chan, W. K., Quantitative stress analysis by means of the thermoelastic effect. *The Journal of Strain Analysis for Engineering Design*, 1985, 20 (3), 129-137.
6. Dulieu-Smith, J. M., Alternative calibration techniques for quantitative thermoelastic stress analysis. *Strain*, 1995, 31 (1), 9-16.
7. Dulieu-Barton, J. M. and Stanley, P., Development and applications of thermoelastic stress analysis. *The Journal of Strain Analysis for Engineering Design*, 1998, 33 (2), 93-104.
8. Stanley, P. and Chan, W. K., The application of thermoelastic stress analysis to composite materials. *Journal of Strain Analysis*, 1988, 23 (3), 137-143.
9. Dulieu-Smith, J. M., Quinn, S., Shenoi, R. A., Read, P. J. C. L., and Moy, S. S. J., Thermoelastic stress analysis of a GRP tee joint. *Applied Composite Materials*, 1997, 4 (5), 283-303.
10. Daniel, I. M. and Ishai, O., *Engineering Mechanics of Composite Materials*. 1994: Oxford University Press.
11. Maldague, X. and Marinetti, S., Pulse phase infrared thermography. *Journal Applied Physics*, 1996, 79 (5), 2694-2698.
12. Drew, R. C. and White, R. G. *An investigation into damage propagation and its effect upon dynamic properties of CFRP composite materials.* In *Proceedings of the Fourth International Conference on Composite Structures*. 1987. Paisley College of Technology.
13. Cunningham, P. R., Dulieu-Barton, J. M., Dutton, A. G., and Shenoi, R. A., The effect of ply lay-up on the thermoelastic repsonse of laminated composites. *Key Engineering Materials*, 2002, 221-222, 325-336.
14. Herakovich, C. T., On the relationship between engineering properties and delamination of composite materials. *Journal of Composite Materials*, 1981, 15 (3), 336-348.
15. Emery, T.R., Identification of damage in composite materials using themoelastic stress analysis. PhD Thesis, *University of Southampton*, May 2007.
16. Marinetti, S., Plotnikov, Y. A., Winfree, W. P., and Braggiotti, A., *Pulse phase thermography for defect detection and visualization*. Nondestructive Evaluation of Aging Aircraft, Airports, and Aerospace Hardware III, ed. Mal, A.K. Vol. 3586. 1999: Proceedings of SPIE.
17. Dulieu-Barton, J. M., Earl, J. S., and Shenoi, R. A., Determination of the stress distribution in foam-cored sandwich construction composite tee joints. *The Journal of Strain Analysis for Engineering Design*, 2001, 36 (6), 545-560.
18. Harwood, N. and Cummings, W.N., Thermoelastic stress analysis. 1991, *New York: Adam Hilger.*